concentrations were dependent upon air mass history; air masses transported from lower latitudes generally had higher peroxide concentrations.

If we take the measured H_2O_2 concentrations of Van Valin et al.[51] and scale the theoretical oxidation rates in Figure 6.11 down accordingly, we still have SO_2 oxidation rates on the order of 100 percent per hour. Of course, such rates have not been observed during WHITEX or elsewhere because the H_2O_2 is used up well before significant quantities of SO_2 are oxidized. Since one mole of H_2O_2 is consumed for each mole of SO_2 oxidized, the average peroxide concentration of 0.3 *ppb* can produce $0.4\mu g/m^3$ of sulfate as sulfur ($1.2\mu g/m^3$ as sulfate). Of course higher concentrations of sulfate can be produced as additional H_2O_2 is produced. Also, if the reactions with the other oxidants in Figure 6.11 are important, additional aqueous-phase oxidation could occur.

Thus, it appears that rapid SO_2 oxidation suggested by the WHITEX data can be supported by theoretical aqueous-phase mechanisms. Although H_2O_2 is not the only oxidant of importance, it has been measured at sufficient concentrations in winter to explain much of the observed sulfate formation. Iron and manganese, which are contained in NGS particulate matter, can catalyze the reaction with dissolved oxygen. Ozone, typically 20 to 40 *ppb* during the winter, can also contribute significantly to aqueous-phase oxidation.

Evidence for aqueous-phase oxidation is available in the particle size distribution data. When particle size distributions were stratified by relative humidity, a larger fraction of the total fine particle mass was in the $0.5\mu m$ size range at the higher humidities. At lower humidities a relatively greater fraction of particles were found in the range 0.1 to 0.3 μm. Hering and Friedlander[52] found that sulfate in Los Angeles consisted of two sizes: (1) one at 0.2 μm, was found to be associated with sulfate formed from gas-phase oxidation and (2) one at 0.5 μm was found to be due to aqueous-phase oxidation. McMurry and Wilson[53] used aerosol growth data versus particle size to infer the relative importance of gas- and aqueous-phase oxidation mechanisms: growth in the 0.5 μm size range resulted mainly from aqueous-phase oxidation. Thus, the particle size data from WHITEX are consistent with the aqueous-phase oxidation mechanism.

The importance of aqueous-phase oxidation is indicated by the particle size data collected during WHITEX and the oxidation rates that are greater than what one would expect from gas-phase oxidation. While it is difficult to determine the relative importance of various aqueous-phase oxidants and catalysts, theoretical and empirical knowledge indicates that SO_2 oxidation rates on the order of 1 percent per hour are plausible for aqueous-phase reactions, but not for gas-phase reactions. Thus, it is not surprising that the empirical fit of SO_2 oxidation rate is proportional to relative humidity. The amount of water associated with hygroscopic aerosol increases with increasing humidity. Also, clouds, fog, and cooling tower plumes are more likely to occur at higher humidities.

6.4 Analysis of Meteorological Conditions

Upper-level winds from Page, Arizona were analyzed to determine possible NGS plume transport patterns. In addition, the ARL-ATAD backward air mass trajectory model was run for the western United States for the period of WHITEX to establish potential regional contributing source areas. Finally, the upper-level Page winds were used to calculate NGS plume parcel positions and ages as a function of time during the WHITEX experiment.

6.4.1 Summary of Upper-level Winds in Page

Table 6.8 summarizes the wind speed and direction measured at 300, 600, and 1000 meters above ground (m agl) for each of the soundings conducted during the WHITEX experiment. Typically,

Table 6.7: Field measurements of SO_2 oxidation rates in power plant plumes (adapted from Seinfeld (1986).

Power Plant and Location	SO_2 Oxidation Rate ($\%/hr$)	Reference
Keystone, Pennsylvania	0–10	Newman *et al.* (1975)[54]
Labadie, Missouri	0.41–4.9	Cantrell and Whitby (1978)[55]
Muscle Shoals, Alabama	0–5	Forrest and Newman (1977)[56]
Four Corners, New Mexico	2–8	Pueschel and Van Valin (1978)[57]
Labadie, Missouri	0–4	Gillani (1978)[37]
		Gillani *et al.* (1978)[58]
		Husar *et al.* (1978)[38]
Cumberland, Tennessee	0–7	Meagher *et al.* (1978)[59]
		Forrest *et al.* (1977)[56]
Alberta, Canada	0–3	Lusis *et al.* (1978)[36]
Keystone, Pennsylvania	0–5	Dittenhoefer and dePena (1978)[60]
Centralia, Washington	0–6	Hobbs *et al.* (1979)[61]
Four Corners, New Mexico	0.15–0.5	Mamane and Pueschel (1980)[62]
Sherburne County, Minnesota	0–5.7	Hegg and Hobbs (1979)[63]
Big Brown, Texas	0.4–14.9	Hegg and Hobbs (1980)[64]
Navajo, Arizona	0–0.8	Richards *et al.* (1981)[35]

soundings were taken three times per day: at 0700 (near sunrise), 1100 (midday), and 1700 (near sunset). Thus, winds are resolved to approximately 6 hour or 12 hour increments throughout the study.

Figure 6.12 shows the time history of wind speed measured at 300, 600, and 1000 meters above ground. The NGS plume centerline is expected to be generally in the layer between 600 and 1000 meters above ground. The 300-meter and 1000-meter elevations characterize transport at lower and upper levels after the NGS plume has diffused vertically. The NGS plume is probably affected by all three levels as it is transported and dispersed in the region. Figure 6.12(a) shows that wind speed increased dramatically on four separate occasions: Julian Days 8, 19, 28, and 44. Wind speed maxima are also seen at the other levels; however, they are most clearly evident at the lower (300 m) level. The high winds are likely the result of the passage of fronts with strong advection especially near the surface. Wind speeds increase with elevation with average wind speeds of 2.8 m/s at 300 meters, 4.5 m/s at 600 meters, and 7.2 m/s at 1000 meters. The vector-average wind speeds over the WHITEX period are much lower (0.8, 0.8, and 2.1 m/s, respectively, for the 300, 600, and 1000 meter levels), which suggests a sloshing (back-and-forth) air motion. The four days with wind speed maxima were used as an initial cut on dividing the WHITEX measurement period into separate time periods.

Figure 6.13 shows the time history of wind direction at the three upper levels in Page during WHITEX. These plots were used in conjunction with the wind speed plots to divide the WHITEX period into the 13 periods shown in Table 6.9. Period 1 (JD 7–8) is characterized by northwesterly winds. Period 2 (JD 9–12) has winds switching initially from northerly to northeasterly. Period 3 (JD 13–16) is characterized by significant wind direction changes but typically southerly transport winds. Period 4 (JD 17–19) is characterized by winds initially from the north and northeast, changing to westerly. Period 5 (JD 20–22), after the front passage, is characterized by north or northeasterly winds at the upper levels with much more variable southerly winds at the 300-meter

Table 6.8: Upper air winds measured in Page, Arizona at three levels (300, 600, 1000 m agl) during the WHITEX study, January–February 1987.

Wind Speed and Wind Direction in Page, AZ

			300 m		600 m		1000 m	
Day	Hour	Time	WS (m/s)	WD	WS (m/s)	WD	WS (m/s)	WD
7	6	7.25	4.5	67.0	4.5	67.0	4.5	67.0
8	6	8.25	5.7	301.0	6.5	302.0	6.5	302.0
8	11	8.46	3.3	307.0	3.2	288.0	1.7	19.0
8	17	8.71	7.4	310.0	5.4	301.0	5.4	302.0
9	6	9.25	2.4	3.0	2.4	3.0	2.4	3.0
9	11	9.46	1.0	48.0	2.5	29.0	6.3	38.0
9	17	9.71	1.9	325.0	3.6	29.0	6.6	49.0
10	6	10.25	1.7	339.0	2.2	330.0	2.2	330.0
10	11	10.46	1.7	107.0	2.3	324.0	3.2	75.0
10	17	10.71	3.2	172.0	2.4	23.0	5.0	54.0
11	6	11.25	1.5	64.0	0.9	57.0	7.5	60.0
11	11	11.46	1.7	79.0	2.2	114.0	9.6	59.0
11	17	11.71	0.7	92.0	5.9	78.0	10.6	80.0
12	6	12.25	3.0	81.0	7.2	65.0	3.4	170.0
12	11	12.46	0.8	301.0	2.2	98.0	6.2	185.0
12	17	12.71	1.3	300.0	4.0	155.0	0.7	84.0
13	6	13.25	0.3	147.0	3.2	127.0	4.7	245.0
13	11	13.46	0.9	161.0	2.8	198.0	4.7	258.0
13	17	13.71	2.5	204.0	4.3	194.0	12.7	277.0
14	6	14.25	3.5	57.0	2.2	19.0	4.2	20.0
14	11	14.46	1.1	203.0	0.2	151.0	5.9	53.0
14	17	14.71	1.9	163.0	2.5	146.0	3.4	234.0
15	6	15.25	1.7	88.0	5.0	134.0	6.6	207.0
15	11	15.46	1.2	133.0	5.2	199.0	10.5	215.0
17	6	17.25	2.8	4.0	4.0	8.0	5.3	12.0
17	11	17.46	2.4	327.0	6.9	12.0	16.8	19.0
17	17	17.71	1.8	64.0	8.0	1.0	11.8	17.0
18	7	18.29	3.9	297.0	2.0	13.0	7.8	11.0
18	17	18.71	2.9	149.0	3.7	219.0	10.0	300.0
19	11	19.46	0.9	96.0	7.2	299.0	9.2	325.0
19	17	19.71	6.1	69.0	8.1	64.0	8.7	48.0
20	6	20.25	7.6	28.0	4.2	41.0	4.0	28.0
20	11	20.46	2.4	133.0	2.3	118.0	7.0	57.0
20	17	20.71	1.2	156.0	3.7	350.0	5.2	4.0
21	6	21.25	1.3	265.0	3.7	350.0	5.2	4.0
21	11	21.46	1.0	198.0	6.0	316.0	8.9	343.0
21	17	21.71	2.5	163.0	2.1	106.0	13.7	326.0
22	6	22.25	1.9	122.0	1.1	154.0	6.7	318.0
22	11	22.46	0.2	208.0	2.0	162.0	4.3	301.0
22	17	22.71	2.3	200.0	5.5	210.0	4.9	275.0
23	6	23.25	3.0	184.0	7.9	166.0	5.6	244.0
23	11	23.46	1.7	54.0	3.8	159.0	7.7	226.0
23	17	23.71	0.8	43.0	0.7	221.0	3.0	296.0
24	7	24.29	1.8	63.0	6.7	275.0	5.7	277.0
24	11	24.46	1.9	159.0	6.7	275.0	5.7	277.0
24	17	24.71	1.9	219.0	5.7	225.0	5.7	277.0
25	7	25.29	1.8	243.0	1.5	244.0	11.8	292.0
25	11	25.46	2.7	190.0	2.6	248.0	11.8	292.0
25	17	25.71	0.8	71.0	5.0	257.0	12.3	282.0
26	6	26.25	0.1	114.0	5.0	227.0	4.8	249.0
26	11	26.46	2.3	217.0	4.3	210.0	5.0	257.0
26	17	26.71	4.6	328.0	4.4	198.0	8.4	272.0

Table 6.8: cont.

			Wind Speed and Wind Direction in Page, AZ					
			300 m		600 m		1000 m	
Day	Hour	Time	WS (m/s)	WD	WS (m/s)	WD	WS (m/s)	WD
27	6	27.25	1.8	233.0	3.1	205.0	4.9	250.0
27	11	27.46	1.1	240.0	4.6	210.0	4.9	250.0
27	17	27.71	2.3	113.0	4.6	181.0	3.7	256.0
28	6	28.25	1.1	114.0	4.9	169.0	11.5	220.0
28	11	28.46	9.6	208.0	16.1	222.0	21.3	239.0
28	17	28.71	14.4	297.0	13.2	279.0	18.5	267.0
29	6	29.25	2.3	102.0	2.2	89.0	4.1	141.0
29	11	29.46	6.1	57.0	7.4	49.0	3.7	136.0
29	17	29.71	4.7	49.0	3.4	47.0	1.6	36.0
30	6	30.25	4.2	54.0	4.0	73.0	7.3	160.0
30	11	30.46	1.8	71.0	2.6	110.0	9.9	167.0
30	17	30.71	1.9	89.0	3.6	115.0	9.6	163.0
31	6	31.25	5.8	7.0	10.0	19.0	16.7	29.0
31	11	31.46	5.9	355.0	10.0	19.0	16.7	29.0
31	17	31.71	2.7	70.0	2.2	338.0	6.9	312.0
32	6	32.25	2.5	331.0	1.7	310.0	4.5	357.0
32	11	32.46	2.1	168.0	2.3	254.0	4.2	272.0
32	17	32.71	1.1	162.0	4.9	204.0	7.8	264.0
33	6	33.25	4.5	222.0	3.4	172.0	5.7	253.0
33	11	33.46	1.2	192.0	5.4	178.0	7.0	195.0
33	17	33.71	1.8	254.0	4.4	198.0	1.8	286.0
34	6	34.25	0.5	190.0	2.7	192.0	10.4	220.0
34	11	34.46	2.1	145.0	3.1	173.0	10.5	217.0
34	17	34.71	0.8	29.0	4.1	329.0	3.6	239.0
35	6	35.25	2.9	355.0	5.8	350.0	8.4	27.0
35	11	35.46	2.0	5.0	6.5	6.0	8.4	27.0
35	17	35.71	3.4	57.0	6.6	66.0	6.8	30.0
36	6	36.25	3.3	56.0	4.5	46.0	7.6	52.0
36	11	36.46	1.5	110.0	3.0	71.0	12.0	48.0
36	17	36.71	1.6	34.0	4.5	28.0	13.1	40.0
37	6	37.25	0.8	6.0	2.4	9.0	10.8	51.0
37	11	37.46	2.1	111.0	4.4	35.0	12.4	54.0
37	17	37.71	3.4	63.0	5.1	66.0	11.2	60.0
38	6	38.25	2.0	298.0	3.1	100.0	4.9	206.0
38	11	38.46	1.4	85.0	3.3	56.0	2.0	135.0
38	17	38.71	1.4	6.0	3.2	76.0	4.2	153.0
39	6	39.25	2.6	70.0	5.3	84.0	6.0	143.0
39	11	39.46	3.8	74.0	9.8	62.0	2.6	169.0
39	17	39.71	0.5	107.0	3.5	134.0	6.5	165.0
40	6	40.25	1.1	48.0	3.7	118.0	6.5	198.0
40	11	40.46	0.3	35.0	3.9	196.0	5.5	199.0
40	17	40.71	2.2	67.0	2.6	15.0	4.8	181.0
41	6	41.25	4.4	184.0	9.0	178.0	4.0	181.0
41	17	61.71	1.6	61.0	0.6	58.0	3.6	318.0
42	6	42.25	3.4	52.0	0.6	58.0	3.6	318.0
42	11	42.46	2.8	40.0	4.7	60.0	2.6	329.0
42	17	42.71	2.7	57.0	2.1	94.0	2.6	329.0
43	6	43.25	1.8	36.0	2.7	65.0	6.6	191.0
43	17	43.71	1.5	155.0	4.2	286.0	6.6	276.0
44	6	44.25	0.6	116.0	3.1	251.0	7.1	255.0
44	11	44.46	1.5	7.0	2.7	201.0	3.8	236.0
44	17	44.71	1.8	58.0	1.4	275.0	5.9	214.0
45	11	45.46	14.2	298.0	18.0	301.0	15.3	300.0
45	17	45.71	17.7	301.0	16.2	300.0	15.3	310.0
46	7	46.29	2.4	334.0	16.2	300.0	15.3	310.0
46	11	46.46	2.4	126.0	4.5	166.0	4.5	162.0
46	18	46.75	2.6	5.0	2.3	355.0	2.7	170.0
47	6	47.25	3.7	325.0	6.6	320.0	15.9	355.0
47	11	47.46	1.9	345.0	4.0	322.0	15.9	355.0
47	17	47.71	6.6	33.0	5.1	34.0	3.4	46.0
48	6	48.25	4.9	303.0	4.1	332.0	3.9	29.0
48	11	48.46	1.6	349.0	1.4	353.0	3.8	55.0
48	17	48.71	2.2	120.0	0.9	151.0	2.6	349.0
49	6	49.25	3	5.0	2.9	74.0	4.2	78.0

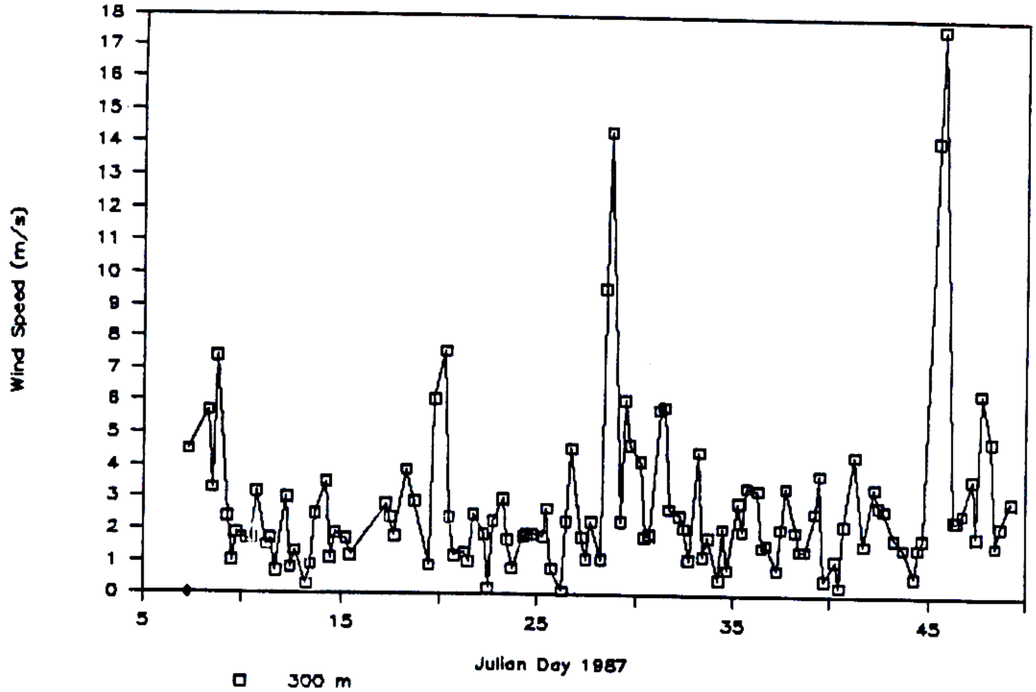

Figure 6.12: Upper-level wind speed measured in Page during WHITEX, January–February 1987. (a) 300 m agl

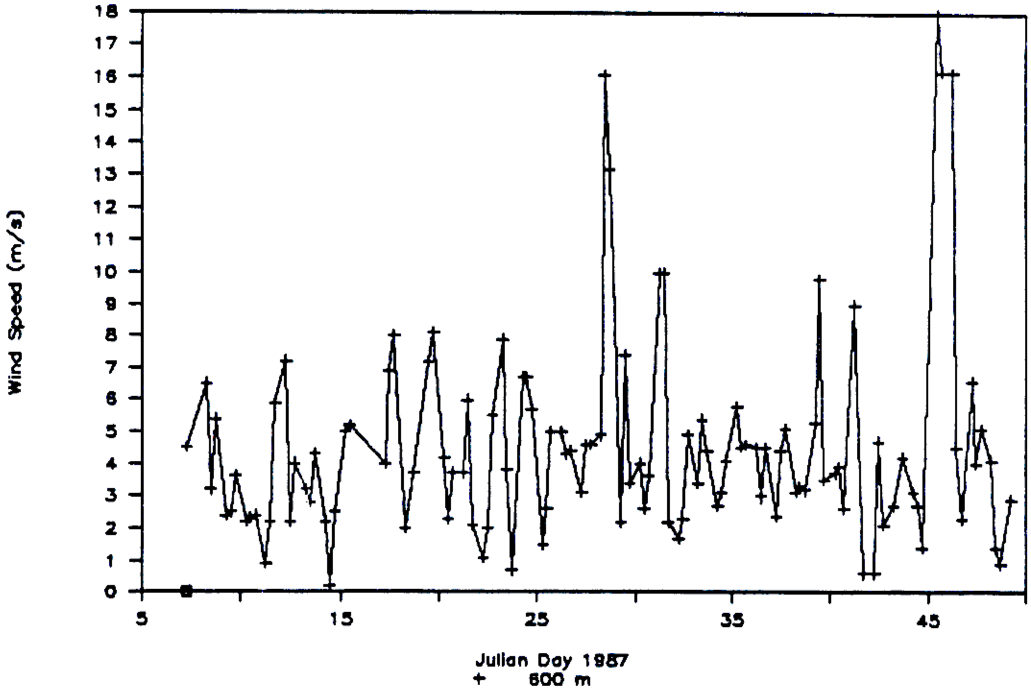

Figure 6.12: Upper-level wind speed measured in Page during WHITEX, January–February 1987. (b) 600 m agl

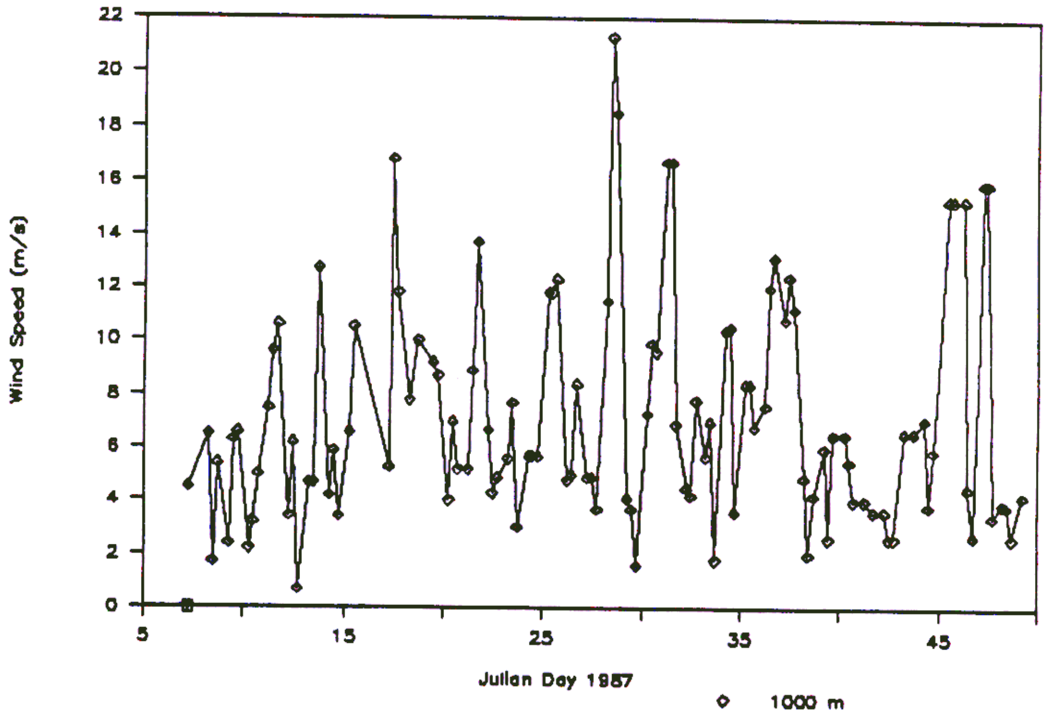

Figure 6.12: Upper-level wind speed measured in Page during WHITEX, January–February 1987. (c) 1000 m agl

height. Period 6 (JD 23–28) is interesting because of its fairly constant southwesterly to westerly upper-level (600 and 1000 m) winds, but with back-and-forth (sloshing) lower-level (300 m) winds. These lower-level winds appear to oscillate between southwesterly and easterly directions. After the front passage on Day 28, Period 7 (JD 29–32) has northeasterly winds with more easterly and southeasterly at the higher levels. Period 8 (JD 33–35) has southwesterly winds, while Period 9 (JD 36–38) has northeasterly winds. Period 10 (JD 39–40) has southerly winds in the upper layers and easterly winds in the lower layer. Period 11 (JD 41–43) has variable winds, with northeasterly and easterly winds at the lower levels and southerly, westerly, and northwesterly winds at the higher levels. During Period 12 (JD 44) lower-level winds are easterly while upper-level winds are southwesterly. After the major front passage at the end of JD 44, Period 13 (JD 45–49) is characterized by rapidly changing wind directions most often in the northerly direction.

Table 6.9: Classification of WHITEX into 13 time periods and their representative wind directions and synoptic meteorological categories.

Period No.	Julian Day	Upper-Air Winds	Synoptic Categories†
1	1–8	NW	4, 1/3, 4, 1/4, 1/2/3, 4, 3/4, 3
2	9–12	NE	4, 4, 4, 4
3	13–16	S	4, 4, 3, 3
4	17–19*	NW-N-NE	3, 4, 4
5	20–22	N-NE	3/4, 4, 4
6	23–28*	SW	3/4, 4, 4, 4, 4, 1/4
7	29–32	NE	4, 4, 3, 4
8	33–35	SW	4, 1/4, 3/4
9	36–38	NE	4, 4, 4
10	39–40	S	4, 4
11	41–43	NE	4, 4, 4
12	44*	SW	4
13	45–49	NW-N-NE	3/4, 4, 3, 3/4, 4

*Front passage

†1 – prefrontal (moderate dispersion),
2 – warm front (moderate dispersion),
3 – postfrontal (excellent dispersion),
4 – polar high (poor dispersion)

The vector-average wind direction during WHITEX was northwesterly to northerly; vector-average wind directions were 3, 336, and 319 degrees (from north), respectively, for the 300, 600, and 1000 meter levels.

6.4.2 Trajectory Analysis

Backward air mass trajectories from the Grand Canyon were calculated for the entire WHITEX period (see Appendix 6G). Trajectories were calculated using the ARL-ATAD model[65] for every 6 hours for the period Julian Day 1 through 50 1987. Trajectories are calculated using average winds in the mixed layer based on an interpolation of National Weather Service upper-air wind measurements in space and in time (every 3 hours). Each trajectory is calculated for a duration of 5 days.

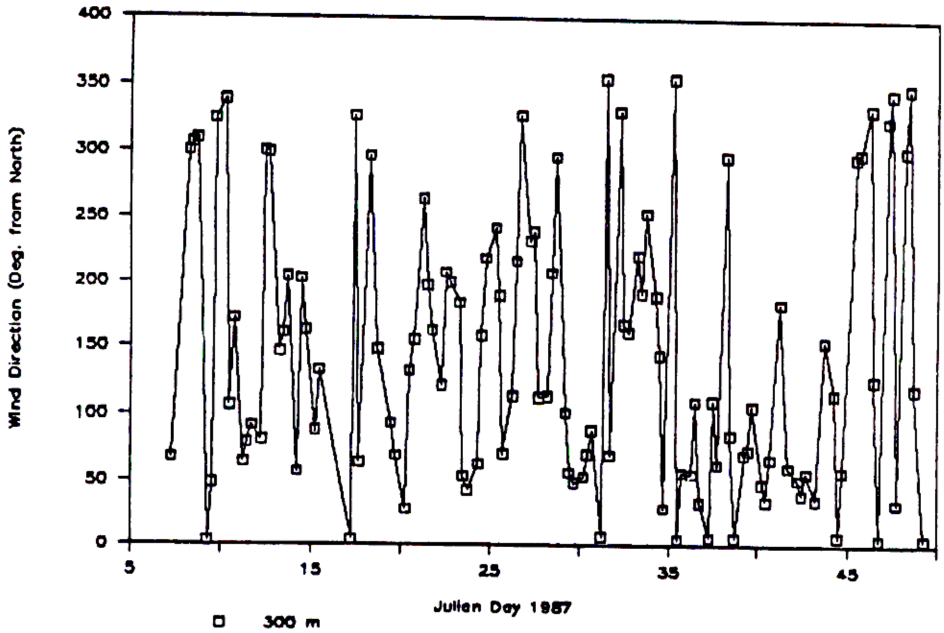

Figure 6.13: Upper-level wind direction measured in Page, Arizona during WHITEX, January–February 1987. Note, since wind directions of 0 deg and 360 deg (north) are the same, some wind

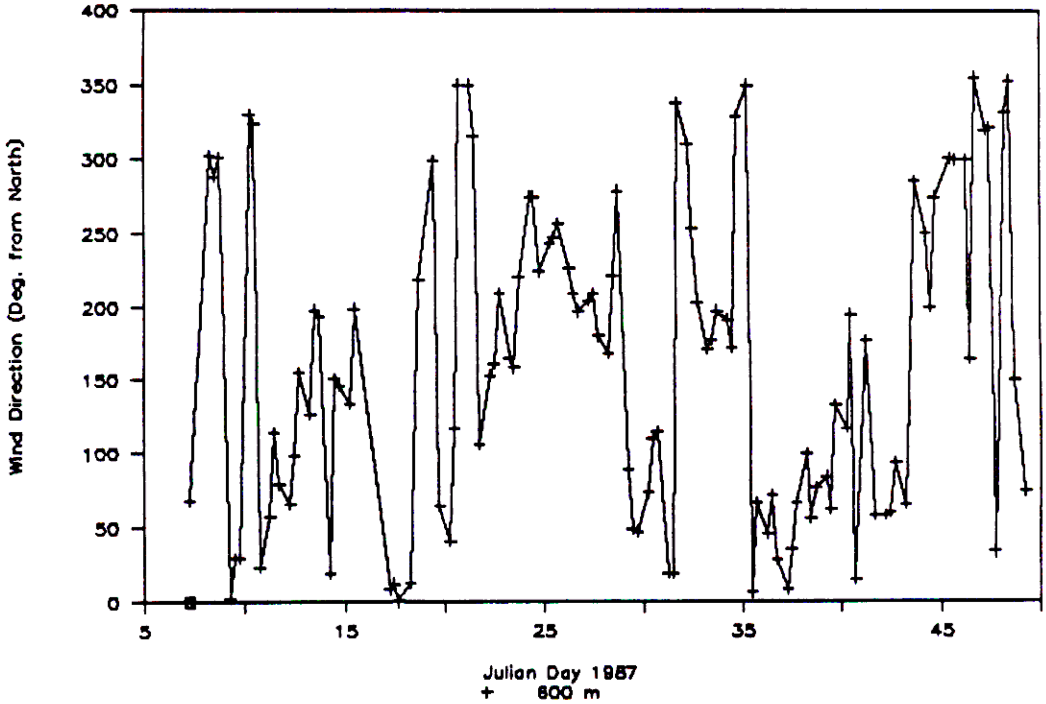

Figure 6.13: Upper-level wind direction measured in Page, Arizona during WHITEX, January–February 1987. Note, since wind directions of 0 deg and 360 deg (north) are the same, some wind direction changes appear magnified in this figure.

(b) 600 m agl

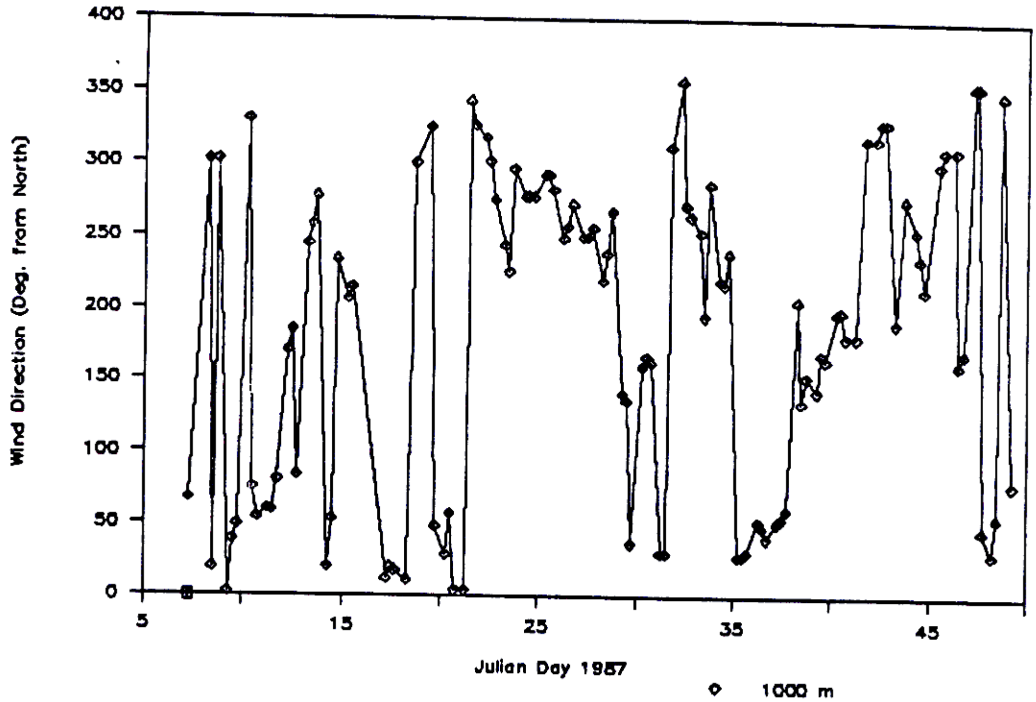

Figure 6.13: Upper-level wind direction measured in Page, Arizona during WHITEX, January–February 1987. Note, since wind directions of 0 deg and 360 deg (north) are the same, some wind direction changes appear magnified in this figure.

(c) 1000 m agl

These trajectories may not accurately portray air parcel movement in the WHITEX area because they are not based on local winds, which may be decoupled from synoptic winds aloft and blocked and channeled by the high terrain of the Lake Powell basin. However, for days in which the WHITEX winds are coupled to flow aloft, they give an indication of potential source areas. In addition, the length of the trajectories reflects the magnitude of the average mixed layer wind speed and the curvature of the trajectories is indicative of wind direction changes.

The trajectories for January 14 and 15, 1987 show recirculation or stagnation in the WHITEX study area. Stagnant conditions are also evident in the trajectories for January 27. Trajectories for February 8 and 9 (Julian days 39 and 40) suggest air masses from the large copper smelter emission sources in southern Arizona could have been influencing the WHITEX region.

6.4.3 Calculation of Potential NGS Plume Position and Age (Streakline Analysis)

The upper-air winds measured in Page during WHITEX (see Table 6.8) were used to calculate the potential position and orientation of the NGS plume centerline as a function of time. Winds at 300 and 600 meters above ground were used to characterize flow in two layers between the effective plume height and the ground. Wind direction and wind speed for each time period were used to calculate plume centerline position by vector addition.

Using vector notation (the underlined variable is a vector), the position of a plume parcel at time t after being emitted at $t = 0$ is simply the product of the vector sum of the winds and the time t:

$$\underline{x} = \underline{v}(0,t)\, t \tag{6.5}$$

where $\underline{x}$ is the location of the plume parcel after transport time t and $\underline{v}(0,t)$ is the vector sum of winds over the period of time from 0 to t. Here the wind vector is defined as the direction in which the wind will carry material (not the conventional direction from which the wind blows).

Streaklines, or the position of the plume centerline, can be plotted as a function of time by connecting points of various age. the position of the oldest plume parcel is a function of the winds that occurred from time of emission ($t = 0$) to the current time. A streakline is different from a trajectory in that a streakline is a "snapshot" of aged plume material at a given time. Hence, it is a function of winds during and prior to the time of interest. A trajectory shows where an emission at a given time is transported in subsequent time.

The assumption made in these calculations is that winds measured in Page are representative of winds at other locations. This assumption is valid only if winds are synoptically influenced (influenced by synoptic pressure gradients) rather than mesoscale influenced (influenced by elevated terrain). These plume centerlines (streaklines) are plotted in Appendix 6H, with plume positions calculated on the basis of 300 and 600 meter winds on facing pages.

In these figures, it is assumed that the wind speed and direction measured at a specific time persisted for the entire previous time period (the time between the previous wind measurement and the current one). Since upper-level winds in Page were typically measured at 0600, 1100, and 1700, the corresponding initial time steps are 13, 5, and 6 hours, respectively. A square is used in the figures to indicate the location of the NGS plume after each time step. The plume age for any given parcel can be estimated by counting the number of squares between the NGS plant site (coordinates 0,0) and the given parcel. Since typically there are three time steps per day (0600, 1100, 1700 hours), a 1-day-old plume would be three squares from NGS, a 2-day old plume would be six squares away, and so forth. Plume centerline positions are calculated for a total of 16 time steps or typically one time step more than 5 days (120 hours).

A clear plastic map showing WHITEX receptor sites and major emission sources is provided in the back of this report. This map can be used to overlay on top of the Appendix 6H figures to determine the potential location of the NGS plume relative to key WHITEX measurement sites. By counting squares, the NGS plume parcel age can be estimated at each location of interest.

Table 6.10 presents our estimates of potential NGS plume parcel age at each WHITEX receptor of interest and for each time period during WHITEX. It was assumed that if either the 300 *m* or 600 *m* plume centerline was at or near a given receptor, that receptor's concentration may have been influenced by NGS emissions. Using typical horizontal dispersion coefficients (see Section 6.4.3), the plume would be expected to be at least 45 degrees wide at each location. If there was significant wind shear (which seems to be the case often during WHITEX), the NGS plume would be even wider. Thus, the plume centerline would not have to be directly over a given receptor for it to be influenced by NGS emissions. If the NGS plume was estimated to be influencing a given receptor, an age was recorded in Table 6.10. If the NGS was not expected to be influencing the receptor, the age is left blank in the table. For the lower level winds (at 300 *m*), if the centerlines suggested transport from NGS to the west, it was assumed that these trajectories would be channeled within the Colorado River drainage basin and likely impact Hopi Point in the Grand Canyon. If a slight modification of winds was required for a plume to intersect a given receptor, the plume ages in Table 6.10 are placed in parentheses. It was also assumed that under almost all conditions the Page receptor would have been influenced by NGS emissions on the order of 6 to 12 hours old because of Page's proximity to NGS. Table 6.11 compares means estimated NGS plume age at sites during WHITEX.

Table 6.12, 6.13, 6.14, 6.15, 6.16, 6.17, 6.18, and 6.19 show the association between sulfate episodes during WHITEX and estimated NGS plume "hits" and elevated concentrations of SO_2 and nitrate. Qualitative judgment was used to determine the episodes by examining the time traces of sulfate at each site. There is a very high degree of association, suggesting that the NGS plume position analysis based on streaklines, although uncertain, is not far off target.

All of the available 6-hour SO_2 and sulfate data from Hopi Point (79 observations) were segregated into two groups: (1) those observations where the NGS plume streakline analysis indicated that the NGS plume was in the area (a "hit") and (2) those observations where the streakline analysis indicated that the NGS plume was not in the area (a "miss").

For sulfate, there were 56 "hits" and 23 "misses". Multi-response permutation procedures (MRPPT) (see Appendix 6J) were applied to this data set. The probability that the association between NGS plume and the concentrations of sulfate could be due to random mechanisms was found to be 4.8 percent. Thus, from the MRPPT it is highly probable that the high sulfate at Hopi Point is correlated with the predicted NGS plume "hit" based on the streakline analysis using Page wind data.

A similar analysis was carried out for SO_2. Here the probability that the association between plume "hits" and SO_2 is due to random processes is 6.0 percent. The MRPPT was also carried out for nitrate; the probability that the association between plume "hits" and nitrate concentration is due to random processes is 10.0 percent.

The MRPPT was also applied to arsenic, which is emitted principally from the smelters and is not a significant constituent of NGS emissions. the probability that the association between arsenic concentrations at Hopi Point and NGS plume "hits" based on the streakline analysis is due to random events is quite high, 77.1 percent, as one might expect.

These analyses suggest that the high concentrations of SO_2, sulfate, and nitrate at Hopi Point are correlated with the predicted presence of the NGS plume.

Table 6.10: Estimated age of the Navajo Generating Station plume (in hours) at various locations in the WHITEX study region, January–February 1987.

Notes
1. If numbers are not presented for given time and place, the NGS plume is not expected to be in the area.
2. If numbers are presented in parentheses (), the NGS plume would be present with minor modifications of winds.

WHITEX Study Period in 1987		Navajo Generating Station Plume Age (hours)					
Day	Hour	Page, Arizona	Hopi Point	Canyonlands & Monticello	Bullfrog Marina & Hite, Utah	Green River, Utah	Mexican Hat, Utah
9	6	6–12					
9	17	6–12	12				
10	6	6–12					
10	17	6–36					
11	6	6–12	36–48				
11	17	6–12	58				
12	6	6–12	(6–72)				
12	17	6–12	(24)				
13	6	6–12	(48)				
13	17	6–12	(0–48)		6–36		
14	6	6–24	(6–48)				
14	17	6–12	(24–60)				
15	6	6–12	(12–24)				
15	17	6–12	24*				
16	6	6–12	25*				
16	17	6–12	60*				
17	6	6–12	(36)				
17	17	6–12	(36)				
18	7	6–12	(6)				
18	17	6–12			6–12	12	12
19	17	6–12	6–48		(24)		
20	6	6–12	6				
20	17	6–12	10–18				
21	6	6–24	24–30				
21	17	6–12	40–48		24–36		
22	6	6–24					
22	17	6–12			10–36		
23	6	6–12	84				
23	17	6–12	96				120
24	7	6–60	(24)	48	48	96	96
24	17	6–12	(36)	120	6		
25	7	6–48		18	24	(72)	
25	17	6–12		(24)	24–36	(84)	10
26	6	6–24		12	48	(96)	
26	17	6–84			72	120	48
27	6	6–12		72	12–(96)	4–120	48
27	17	6–12		60	120	20–120	48
28	6	6–(36)		96	72–120	132	(96)

*Based on Surface Winds

Table 6.10: cont.

WHITEX Study Period in 1987		Navajo Generating Station Plume Age (hours)					
Day	Hour	Page, Arizona	Hopi Point	Canyonlands & Monticello	Bullfrog Marina & Hite, Utah	Green River, Utah	Mexican Hat, Utah
28	17	6–12		(36)			
29	6	6–12	(12)	48	(48)		(48)
29	17	6–(72)	6–(54)	48–(120)			120
30	6	6–(120)	12–96				
30	17	6–12	60–120				
31	6	6–12					
31	17	6–12	(12)				
32	6	6–12	(132)				
32	17	6–(24)	(30)		12		24
33	6	6–(48)	(132)	40	6	24–30	48
33	17	6–(48)	(48–72)	48	48	48	60
34	6	6–60	84	60	72	20–48	72
34	17	6–(36)	96	72	24–(36)	30–(60) 84	
35	6	6–(48)	(24)	60–72	48–60	(60–72)	90
35	17	6–60	10–(60)	96	72	(72)	96
36	6	6–96	96–120				
36	17	6–(120)	6–120				
37	6	6–(120)	6–120				
37	17	6–12	(12–36)				
38	6	6–(24)	48–(132)				
38	17	6–(12)	36–60				
39	6	6–12	36–(48)				
39	17	6–12	(6)				
40	6	6–12	(24)				
40	17	6–12	(24–36)				
41	6	6–12					
41	17	6–12					
42	6	6–12	(18)				
42	17	6–12	(12–30)				
43	6	6–12	12				
43	17	6–(24)	30–(48)				
44	6	6–(120)	(96)	120	12–(96)	(132)	12–(96)
44	17	6–(120)	(48)	24–(96)	10–(120)	(132)	(96)
45	11	6–12					
45	17	6–12					
46	7	6–12					
46	18	6–12	(12–24)				
47	6	6–12					
47	17	6–12	6–12				
48	6	6–12					
48	17	6–24					
49	6	6–12	24–(30)				

Table 6.11: Comparison of mean estimated NGS plume age (hours) at sites during WHITEX, January–February 1987.

Period No.	Julian Day	Upper-air Winds	Page	Hopi	Canyonlands	Bullfrog	Hite	Gr. River	Mex. Hat	Monticello
1	1–8	NW	—	—	—	—	—	—	—	—
2	9–12	NE	11	36	—	—	—	—	—	—
3	13–16	S	10	31	—	21	21	—	—	—
4	17–19*	NW-N-NE	9	23	—	17	17	12	12	—
5	20–22	N-NE	11	23	—	28	28	—	—	—
6	23–28*	SW	17	60	56	54	54	92	67	56
7	29–32	NE	19	53	56	36	36	—	72	56
8	33–35	SW	27	71	61	42	42	47	69	61
9	36–38	NE	37	65	96	72	72	72	96	96
10	39–40	S	9	28	—	—	—	—	—	—
11	41–43	NE	10	20	—	—	—	—	—	—
12	44*	SW	47	77	120	54	54	132	54	120
13	45–49	NW-N-NE	15	26	60	65	65	132	96	60
Overall			17	46	62	44	44	76	67	62

*Front passage

Table 6.12: Sulfate episodes during the WHITEX study, January-February 1987 at Glen Canyon National Recreation Area (Page,Arizona). Parentheses indicate that a slight modification in winds would be required for the NGS plume to impact the site.

Julian Day 1987	NGS Plume	CD_4	SO_2	NO_3
8 – 9	Yes	—*	No	Yes
12 – 14	Yes	—	Yes	Yes
15 – 17	Yes	Yes	No	Yes
21 – 25	Yes	—	Yes	Yes
27 – 28	Yes	Yes	Yes	Yes
31 – 36	Yes	Yes	Yes	Yes

ast CD_4 Not Analyzed

Table 6.13: Sulfate episodes during the WHITEX study, January-February 1987 at Hopi Point, Grand Canyon National Park. Parentheses indicate that a slight modification in winds would be required for the NGS plume to impact the site.

Julian Day 1987	NGS Plume	CD_4	SO_2	NO_3
8 – 9	No	(Yes)	No	No
11	Yes	—	Yes	No
14 – 17	Yes	Yes	Yes	Yes
19 – 21	Yes	—	Yes	Yes
23	Yes	—	Yes	Yes
27 – 30	No	—	Yes	(Yes)
31	Yes	—	No	Yes
34 – 36	Yes	Yes	Yes	Yes
39 – 44	Yes	Yes	(Yes)	Yes

Table 6.14: Sulfate episodes during the WHITEX study, January-February 1987 at Canyonlands National Park. Parentheses indicate that a slight modification in winds would be required for the NGS plume to impact the site.

Julian Day 1987	NGS Plume	CD_4	SO_2	NO_3
8 – 11	No	(No)	Yes	Yes
13 – 15	No	No	Yes	(Yes)
16 – 17	No	No	No	Yes
19	No	—	Yes	Yes
21 – 25	Yes	—	Yes	Yes
26 – 27	Yes	—	Yes	Yes)
31 – 36	Yes	Yes	Yes	Yes
38 – 40	No	—	Yes	Yes
41 – 44	Yes	Yes	No	(Yes)
46	No	—	No	No
47 – 48	No	—	No	Yes

Table 6.15: Sulfate episodes during the WHITEX study, January-February 1987 at Bullfrog, Utah. Parentheses indicate that a slight modification in winds would be required for the NGS plume to impact the site.

Julian Day 1987	NGS Plume	CD_4	SO_2	NO_3
8 – 10	No	—	No	Yes
11 – 14	No	No	No	Yes
15 – 16	No	No	No	Yes
22 – 25	Yes	—	Yes	Yes
28	Yes	—	Yes	Yes
31 – 35	Yes	Yes	Yes	Yes
41 – 44	(Yes)	Yes	(Yes)	Yes
47 – 48	No	—	No	Yes

Table 6.16: Sulfate episodes during the WHITEX study, January-February 1987 at Hite, Utah. Parentheses indicate that a slight modification in winds would be required for the NGS plume to impact the site.

Julian Day 1987	NGS Plume	CD_4
9	No	—
10 – 11	No	—
14	Yes	—
17	No	—
19	Yes	—
22 – 27	Yes	—
31 – 35	Yes	—
41 – 44	(Yes)	Yes
47 – 48	No	—

Table 6.17: Sulfate episodes during the WHITEX study, January-February 1987 at Green River, Utah. Parentheses indicate that a slight modification in winds would be required for the NGS plume to impact the site.

Julian Day 1987	NGS Plume	CD_4
9 – 10	No	—
14	No	No
17	No	No
19	Yes	—
21 – 22	No	—
24 – 27	Yes	—
31	No	Yes
34	Yes	Yes
35	Yes	Yes
41 – 44	(Yes)	(Yes)
47 – 48	No	—

Table 6.18: Sulfate episodes during the WHITEX study, January-February 1987 at Mexican Hat, Utah. Parentheses indicate that a slight modification in winds would be required for the NGS plume to impact the site.

Julian Day 1987	NGS Plume	CD_4
13	No	—
19 – 20	Yes	—
23 – 24	Yes	—
26 – 27	Yes	—
31	Yes	Yes
35	Yes	Yes
39 – 40	No	—
42 – 43	(Yes)	Yes
47 – 48	No	—

Table 6.19: Sulfate episodes during the WHITEX study, January-February 1987 at Monticello, Utah.

Julian Day 1987	NGS Plume	CD_4
9 – 10	No	—
13 – 15	No	—
17	No	—
19 – 20	No	—
23 – 25	Yes	—
26	No	—
28	Yes	—
30	Yes	—
32	No	—
34 – 35	Yes	Yes
41 – 44	(Yes)	(Yes)
47 – 48	No	—

6.4.4 Summary of Meteorological Analysis of WHITEX Study Period

Table 6.20 summarizes the breakdown of the WHITEX study period into the thirteen time periods, and for each day, the synoptic meteorology, the direction from which the ARL-ATAD trajectory approaches Grand Canyon, the wind direction at three altitudes in Page, the wind speed at 600 meters above ground in Page, and the position of NGS plume material relative to NGS on the basis of the plume centerline (streakline) calculations.

On some days winds are so variable that wind directions cannot be identified. These days are indicated by a dash (- -).

There is considerable wind shear indicated in the Page winds. However, the Page winds are often consistent with the winds derived from the analysis of synoptic weather maps and from the ATAD trajectories.

It is striking to note that NGS plume material is often predicted to be spread over much of the area at the same time. This is due to the wind shear and the variable wind directions exhibited during WHITEX.

6.5 Spatial and Temporal Trends in Sulfates

In this section we analyze the spatial and temporal trends in the measured, sulfate concentrations in the WHITEX study region during January and February 1987. The spatial and temporal trends analysis will also use the measured meteorology and the estimated NGS plume parcel age derived from the measured winds, as well as a spatial eigenvector analysis to make inferences regarding potential contributing sources.

6.5.1 Discussion of Sulfate Time Histories

The time histories of the ammonium sulfate concentrations at all of the WHITEX sites are shown in Figure 4.3. An examination of this figure shows that there are periods of relatively uniform